Functional Analysis and Modeling of a Conformationally Constrained Arg-Gly-Asp Sequence Inserted into Human Lysozyme

Takao Yamada, Atsuko Uyeda, Akinori Kidera, and Masakazu Kikuchi*

Protein Engineering Research Institute, 6-2-3, Furuedai, Suita, Osaka 565, Japan

Received May 27, 1994; Revised Manuscript Received July 25, 1994®

ABSTRACT: To examine the effect of a conformational constraint introduced into the Arg-Gly-Asp (RGD) sequence on cell adhesion activity, we have constructed mutant proteins by inserting RGD-containing sequences flanked by two Cys residues between Val74 and Asn75 of human lysozyme. CRGDC-, CRGDSC-, and CGRGDSC-inserted mutant lysozymes were expressed in yeast, purified, and designated as Cys-RGD3, Cys-RGD4, and Cys-RGD5, respectively. In baby hamster kidney cells, these mutants were shown to possess high cell adhesion activity by interaction with vitronectin receptor (integrin $\alpha_v\beta_3$), and this activity is 2–3-fold higher than that of the RGDS-inserted mutant lysozyme, RGD4. The mutant proteins also inhibited the binding of human fibrinogen to its receptor (integrin $\alpha_{IIb}\beta_3$) at a lower concentration than the RGD4 protein. Peptide mapping and mass spectrometric analyses showed that the two inserted Cys residues in these mutants are linked to each other without any effects on the mode of the four disulfide bonds present in native human lysozyme. These results suggest that the introduction of a conformational constraint into the RGD region significantly increases the cell adhesion activity. The conformation of the RGD region in Cys-RGD4 was modeled by a Monte Carlo simulation. Most of the sampled conformations were grouped into three classes; the first is characterized by an extended Gly conformation, the second assumes a type II′ β turn, and the third has a salt bridge between Arg and Asp. The probability of occurrence in the simulation, as well as the crystal structure of RGD4, suggests that the most probable conformation of RGD belongs to the first class.

The Arg-Gly-Asp (RGD)[1] sequence is well-known as a site in cell adhesive proteins, such as fibronectin (Pierschbacher & Ruoslahti, 1984), vitronectin (Suzuki et al., 1985), and fibrinogen (Watt et al., 1979), for binding to their receptors, the integrins (Hynes, 1987; Hemler, 1991). In addition to these cell adhesive proteins, a number of proteins have been found to contain the RGD sequence, but only a limited number of them possess cell adhesion activity. This fact could be explained by the idea that only an RGD sequence with an appropriate conformation can interact with the receptor molecule (Ruoslahti & Pierschbacher, 1987). To determine the functional conformation of the RGD sequence, we previously constructed mutant proteins by inserting the RGD-containing sequence of human fibronectin between Val74 and Asn75 of human lysozyme, using a yeast expression system (Yamada et al., 1993). We have already reported the structural features of these mutant lysozymes by X-ray crystallographic and two-dimensional NMR techniques and discussed the functional conformation of the RGD sequence (Yamada et al., 1993).

Pierschbacher and Ruoslahti (1987), the first to identify the RGD sequence as a binding site of human fibronectin to the receptor (Pierschbacher & Ruoslahti, 1984), have reported that Gly-Pen-Gly-Arg-Gly-Asp-Ser-Pro-Cys-Ala (where Pen is penicillamine), an RGD-containing peptide with a disulfide bond between the Pen and Cys residues, can inhibit the attachment of normal rat kidney cells to vitronectin more effectively than a linear peptide, GRGDSPC. More recently, Kumagai et al. (1991) have described that cyclo(GRGDSPA) is a much better inhibitor of the attachment of B16 melanoma cells to vitronectin or fibronectin than the linear counterpart, GRGDSPA. These experimental results suggest that the introduction of a conformational constraint into an RGD-containing peptide increases the affinity to the integrin receptor.

To examine whether this observation is also the case in an RGD-containing protein, we have tried to insert an RGD-containing sequence flanked by two Cys residues between Val74 and Asn75 of human lysozyme. This is because a protein and a peptide are naturally different in that the former assumes a definite conformation, in contrast to the latter. Here we report the successful formation of a new disulfide bond between the inserted Cys residues in these mutant lysozymes and their functional evaluation. The modeling of the RGD conformation in these mutants by a Monte Carlo simulation is also shown.

MATERIALS AND METHODS

Vector Constructions. Oligonucleotides were chemically synthesized using an automated DNA synthesizer (Model 380B, Applied Biosystems). The double-stranded DNA encoding CRGDSC, for example, was obtained by annealing 5′-TGCCGCGGTGATTCTTGT-3′ and 5′-ACAAGAATCACCGCGGCA-3′. M13mpXhLZM was ligated with the CRGDSC-coding gene after digestion with *Hin*cII (Yamada et al., 1993). The sequence of the mutant gene thus obtained was confirmed by dideoxy sequencing. The genes encoding the signal sequence and the mutated human lysozyme were combined with an *Xho*I–*Sma*I large fragment from pERI8602 (Taniyama et al., 1988) to construct the expression plasmid.

Expression and Purification of Mutant Lysozymes. Mutant human lysozymes were expressed in yeast as described

* Author to whom correspondence should be addressed.

® Abstract published in *Advance ACS Abstracts,* September 1, 1994.

[1] Abbreviations: RGD, Arg-Gly-Asp; BHK, baby hamster kidney; HEL, human erythroleukemia; BSA, bovine serum albumin; PTH, phenylthiohydantoin; ESI, electrospray ionization; FAB, fast-atom bombardment; MC, Monte Carlo; DTNB, dithiobis(2-nitrobenzoic acid); NMR, nuclear magnetic resonance.

0006-2960/94/0433-11678$04.50/0

previously (Yoshimura et al., 1987). Secreted mutant lysozymes were purified essentially as described (Taniyama et al., 1990). HPLC was performed using a cation-exchange column (Asahipak ES-502C, Asahikasei Co. Ltd., Japan) and a hydroxyapatite column (TAPS-020810, Tonen K. K., Japan).

Measurement of Activity. Lytic activity was measured using *Micrococcus lysodeikticus* cells (Sigma) as a substrate (Taniyama et al., 1990). Protein was determined by measuring the weight in the freeze-dried form of each mutant lysozyme.

Cell adhesion activity was determined using BHK cells as described (Maeda et al., 1989; Yamada et al., 1993). The amount of lysozyme adsorbed onto a plate was estimated by subtracting the unadsorbed amount from the added amount of lysozyme in the assay. The unadsorbed amount was determined from the lytic activity remaining in the sample solution after binding to the plate. The results indicated that the adsorption efficiency was in the range of 60–80% at the concentrations shown in Figure 1, regardless of native and mutant lysozymes.

Purification of Integrin $\alpha_{IIb}\beta_3$ from Human Erythroleukemia Cell Line HEL. The proteins containing integrin $\alpha_{IIb}\beta_3$ were extracted by incubating HEL cells (HEL 92.1.7; ATCC TIB 180) with a 1% Triton X-100 solution, as described (Fitzgerald et al., 1985). The integrin $\alpha_{IIb}\beta_3$ was purified by chromatography on columns of Con A–Sepharose, GRGD-SPK–Sepharose, and Sephacryl S-300. After these steps, highly purified integrin $\alpha_{IIb}\beta_3$ was obtained with a yield of 1 mg/10 L of culture medium.

Binding Assay. The inhibitory effects of mutant lysozymes on the binding of fibrinogen to immobilized integrin $\alpha_{IIb}\beta_3$ were examined using a slight modification of the method of Charo et al. (1991). The integrin $\alpha_{IIb}\beta_3$ (0.1 mg/mL) was diluted 1:100 with a Triton X-100-free solution containing 20 mM Tris–150 mM NaCl–1 mM $CaCl_2$–0.02% NaN_3, pH 7.4, added to 96-well EIA/RIA plates (Costar Corp., Cambridge, MA) at 0.1 mL (0.1 μg) per well, and incubated overnight at 4 °C. To block nonspecific binding, the wells were incubated with 0.15 mL of 50 mM Tris–100 mM NaCl–2 mM $CaCl_2$–0.02% NaN_3–35 mg/mL BSA, pH 7.4, for 2 h at 30 °C, followed by two washes with buffer A (50 mM Tris–100 mM NaCl–2 mM $CaCl_2$–0.02% NaN_3–1 mg/mL BSA, pH 7.4). Biotinylated fibrinogen, prepared as described (Charo et al., 1991), was added at a final concentration of 1 nM in 0.1 mL of buffer A per well and incubated for 3 h at 30 °C in the presence of different concentrations of mutant lysozymes. After two washes with buffer A, bound fibrinogen was quantitated as described (Charo et al., 1991). Nonspecific binding was measured by determining the binding of biotinylated fibrinogen to BSA-coated wells, which was less than 10%.

Peptide Mapping Analysis. Purified Cys-RGD4 (0.25 mg) was dissolved in 0.5 mL of 0.025 N HCl and digested with 1 μg of pepsin (Sigma) at 37 °C for 8 h (Taniyama et al., 1990). Thermolysin digestion was carried out in 0.5 mL of 10 mM Tris–2 mM $CaCl_2$, pH 7.8, with 2 μg of thermolysin (Seikagaku-kogyo K. K., Japan) at 50 °C for 15 h (Yamada et al., 1994). Elastase digestion was performed in 0.5 mL of 0.1 M Tris, pH 8.0, containing 10 μg of elastase (Elastin Products, Owensville, MO) at 37 °C for 1.5 h (Kanaya & Kikuchi, 1992). In each case, the resultant peptides were separated by reverse-phase HPLC equipped with a Shodex ODSpak F-411/S column (Showa-dencoh K. K., Japan) (Taniyama et al., 1990).

Analysis of N-Terminal Amino Acid Sequence. N-Terminal amino acid sequence was determined by using an Applied Biosystems Model 477A sequencer equipped with a 120A on-line PTH-amino acid analyzer.

Table 1: Production and Relative Lytic Activity of Each Mutant Lysozyme

lysozyme	inserted sequence[a]	productivity[b] (mg/L)	relative lytic activity (%)
native		4.2	100
Cys-RGD3	CRGDC	1.5	90
Cys-RGD4	CRGDSC	1.7	97
Cys-RGD5	CGRGDSC	1.4	92

[a] Inserted between Val74 and Asn75 of human lysozyme. [b] Based on lytic activity in the culture supernatant.

Analysis of Amino Acid Composition. The amino acid composition was determined on a 24-h hydrolysate with 6 N HCl at 110 °C in the presence of 4% thioglycolic acid. Amino acid analysis using ninhydrin was performed on a Hitachi Model 835 amino acid analyzer.

Mass Spectrometry. The electrospray ionization (ESI) (Whitehouse et al., 1985) mass spectrum was measured with a JEOL JMS-HX110/110A double-focusing mass spectrometer equipped with an ESI ion source (Analytica, Branford, CT) (Yamada et al., 1994). Each of the mutant lysozymes (10 μg) was dissolved in 50 μL of H_2O–acetic acid–acetonitrile (5:1:4) and infused into the ion source at a flow rate of 1 μL/min.

The fast-atom bombardment (FAB) mass spectrum was obtained using the above spectrometer equipped with a FAB ion source (Kikuchi et al., 1990). The sample (0.5 nmol) was dissolved in water–acetonitrile (1:1), mixed with a liquid matrix [a mixture of dithiothreitol and dithioerythritol (5:1 w/w)], and bombarded with xenon atoms accelerated at a 6-kV potential in the ion source.

Monte Carlo Simulation. Monte Carlo (MC) simulations of two peptide fragments, AVCRGDSCNA (the RGD region in Cys-RGD4) and AVRGDSNA (the RGD region in RGD4) were carried out in the dihedral angle space (Wako & Gō, 1987) with the ECEPP/2 force field (Sippl et al., 1984) at 1000 K. In order to improve the acceptance ratio of forming the ring structure of Cys-RGD4, we adopted the scaled collective variable Monte Carlo method (Noguti & Gō, 1985). This method effectively samples conformations that satisfy the ring closure of the disulfide bond between the two Cys residues. The high-temperature simulation allows sampling of all possible conformations. A total of 10^7 MC steps were accumulated for each peptide.

RESULTS

We obtained three mutant lysozymes, Cys-RGD3, Cys-RGD4, and Cys-RGD5, by inserting CRGDC, CRGDSC, and CGRGDSC sequences, respectively, between Val74 and Asn75 of human lysozyme. The productivity of these proteins in our yeast expression system was estimated by measuring lytic activity in the culture supernatant of each yeast transformant. As shown in Table 1, mutant lysozymes were successfully secreted, although the productivity was lower as compared with that for native lysozyme. Table 1 also shows the relative lytic activities of these mutant lysozymes, using *M. lysodeikticus* as a substrate. Their relative activities were nearly the same as that of the native protein, indicating that the insertion between Val74 and Asn75 has no effect on the active cleft of human lysozyme. The successful folding of these fully active mutants is probably due to the distant location of the insertion site from the active cleft (Inaka et al., 1991).

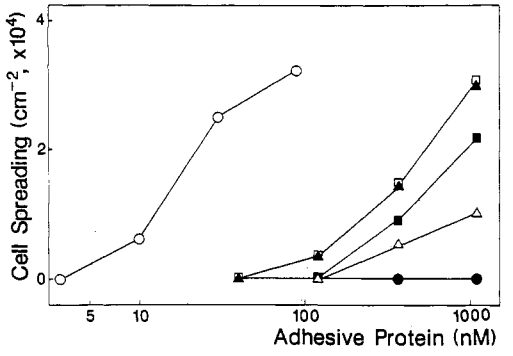

FIGURE 1: Quantitative cell spreading assay on the substrates coated with each mutant lysozyme. The plastic substrates were coated with different concentrations of vitronectin (○), native lysozyme (●), Cys-RGD3 (□), Cys-RGD4 (▲), Cys-RGD5 (■), and RGD4 (△). BHK cells were incubated on the substrates for 60 min in a CO_2 incubator. The extent of cell spreading was expressed as the number of cells adhered to the unit surface area (square centimeters).

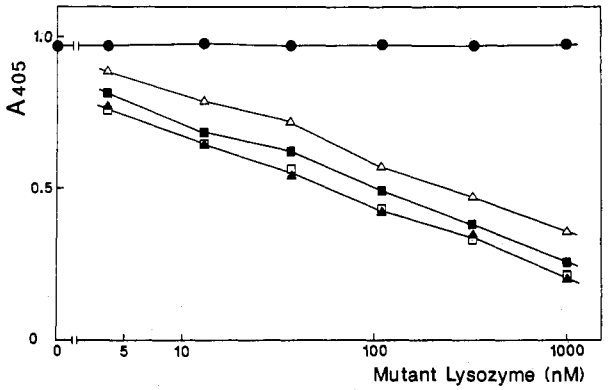

FIGURE 2: Inhibitory effect of each mutant lysozyme on the binding of fibrinogen to integrin $\alpha_{IIb}\beta_3$. The plastic substrates were coated with 1 μg/mL integrin $\alpha_{IIb}\beta_3$, and 1 nM biotinylated fibrinogen was incubated on the substrates for 3 h at 30 °C in the presence of different concentrations of native lysozyme (●). Cys-RGD3 (□), Cys-RGD4 (▲), Cys-RGD5 (■), and RGD4 (△).

The measurement of cell adhesion activity was carried out using BHK cells. As shown in Figure 1, both Cys-RGD3 and Cys-RGD4 possessed quite high activity, which was approximately 5–10% of vitronectin activity. Cys-RGD5 exhibited somewhat lower cell adhesion activity. It was also confirmed that the activities of these mutant lysozymes are 2–3-fold higher than that of the RGDS-inserted mutant lysozyme, RGD4 (Figure 1). The cell adhesion activities of the mutant lysozymes were completely inhibited by the addition of either GRGDSP peptide or polyclonal antibody against vitronectin receptor, as was the case for the vitronectin activity (data not shown). The results suggest that the cell adhesion signals in these mutant proteins are transduced to BHK cells through interaction with the vitronectin receptor, the integrin $\alpha_v\beta_3$. In addition, we examined the effects of these mutant lysozymes on a different integrin than $\alpha_v\beta_3$. For this purpose, we purified the integrin $\alpha_{IIb}\beta_3$ protein from human erythroleukemia cell line HEL (Kieffer et al., 1991) and established a binding assay system using the integrin $\alpha_{IIb}\beta_3$ and biotinylated fibrinogen, as described in Materials and Methods. The binding assay showed that each mutant lysozyme inhibits the binding activity of human fibrinogen in a dose-dependent fashion (Figure 2). Figure 2 also suggests that these mutants are effective in the following order: Cys-RGD3, Cys-RGD4 > Cys-RGD5 > RGD4, which is in good accordance with the aforementioned results on the adhesion assay with BHK cells.

To reveal whether the two Cys residues inserted in these mutant lysozymes are indeed linked to each other, the following analyses were carried out. On the electrospray mass spectrometric analysis, each mutant lysozyme produced several ion signals with multiple charges, as shown in Figure 3. These ion signals for Cys-RGD3, Cys-RGD4, and Cys-RGD5 gave calculated average molecular weights of 15227.6 ± 1.8, 15313.8 ± 1.5, and 15370.4 ± 1.6, respectively, which are consistent with their theoretical molecular weights (15225.4, 15312.4, and 15369.5), indicating that no modification occurs on these mutant molecules. In addition, no free thiol group was detected in these mutants by the DTNB method (Ellman, 1959). These results demonstrate that all of the 10 Cys residues in these mutant lysozymes are linked via five disulfide bonds.

To confirm the locations of the disulfide bonds, peptide mapping analyses were performed on the Cys-RGD4 protein. When subjected to pepsin digestion, the peptide fragments had almost the same retention times on reverse-phase HPLC (Figure 4A) as those derived from the RGD4 protein (Yamada et al., 1994). Particular attention was paid to peptide fragment P (Figure 4A), corresponding to the peptide containing the RGD region in the RGD4 protein. The amino acid analysis, as well as the N-terminal sequence analysis, indicated that fragment P is the large molecule shown in Figure 4B. When digested by thermolysin, fragment P yielded fragment T1 containing Cys65 and Cys81, as well as fragment T2 containing the two inserted Cys residues, Cys77, and Cys95 (Table 2). The low recovery of fragment T1 could be explained by the fact that other fragments containing Cys65 and Cys81 were also detected in the thermolysin digests (data not shown). Fragment T2 was further digested with elastase, resulting in the formation of fragment E, AVCRGDSCNA, with high recovery (Table 2). In addition, fragment E1 containing Cys77 and Cys95 was obtained by elastase digestion of fragment P, although we failed to detect a fragment containing Cys77 and Cys95 among the elastase digests of fragment T2. These results (summarized in Table 2) suggest that the two Cys residues situated at both sides of the RGD sequence in the Cys-RGD4 protein form a disulfide bond, as is the cases for Cys65 and Cys81 and for Cys77 and Cys95. The presence of the new disulfide bond in the Cys-RGD4 protein was further confirmed by fast-atom bombardment mass spectrometry of fragment E (data not shown).

Monte Carlo (MC) simulations of two peptide fragments, AVRGDSNA (the RGD region in RGD4) and AVCRGDSCNA (the RGD region in Cys-RGD4), were carried out at 1000 K to accumulate 10^7 MC steps. When each residue of RGD in AVRGDSNA was assigned to one of the 16 regions (see Figure 5D) of the (ϕ,ψ) map (Zimmerman et al., 1977), 2955 different conformations were found in the record of 10^7 MC steps. These correspond to 72% of 16^3 (=4096) possible combinations of the RGD conformations. On the other hand, the RGD conformations of AVCRGDSCNA were limited to only 915 different combinations (22% of 16^3). Thus, the simulation suggests that the disulfide bond between the two Cys residues confines the RGD conformations to 30% (915/2955).

To characterize the confined conformations of AVCRGDSCNA, we classified them in terms of the (ϕ,ψ) region of the Gly residue (Zimmerman et al., 1977). This classification is consistent with a cluster analysis of RGD conformations in terms of the root-mean-square deviation, because the conformation is mostly determined by the (ϕ,ψ) angles of Gly. Most of the RGD conformations were grouped into the following three classes, each of which has a characteristic distance d between the C_β of Arg and the C_β of Asp: (class 1) d = 9.0–9.5 Å; Gly conformation = E, F, E*, or F*;

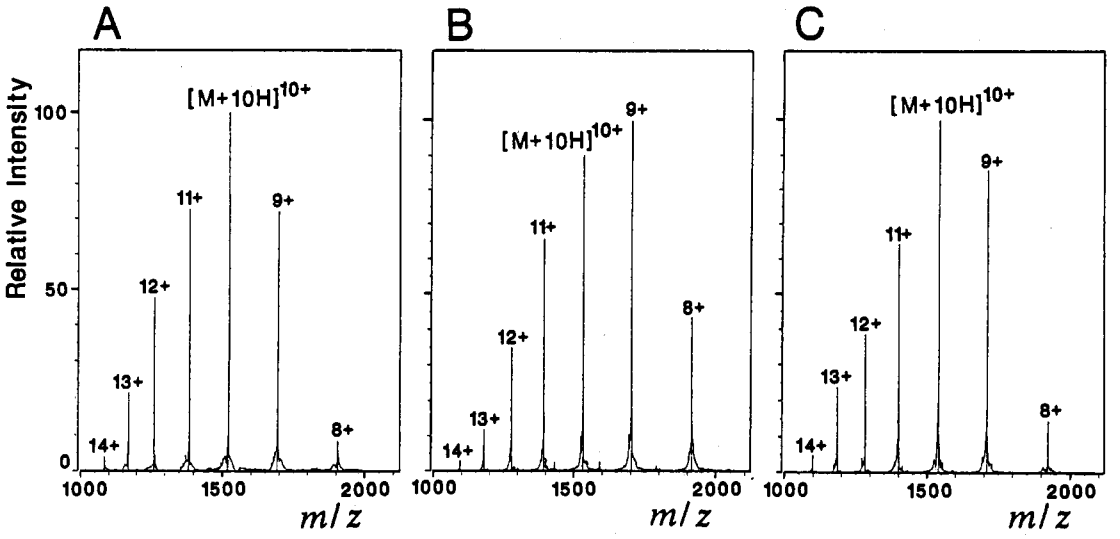

FIGURE 3: Electrospray mass spectra of Cys-RGD3 (A), Cys-RGD4 (B), and Cys-RGD5 (C). The mutant lysozymes produced their respective multiply-charged ion signals ($[M + nH]^{n+}$). For example, the $[M + 10H]^{10+}$ ion signals from Cys-RGD3, Cys-RGD4, and Cys-RGD5 possessed m/z values of 1523.8, 1532.5, and 1538.2, respectively. The mass of each mutant lysozyme was calculated from the m/z values of a series of the multiply-charged ion signals.

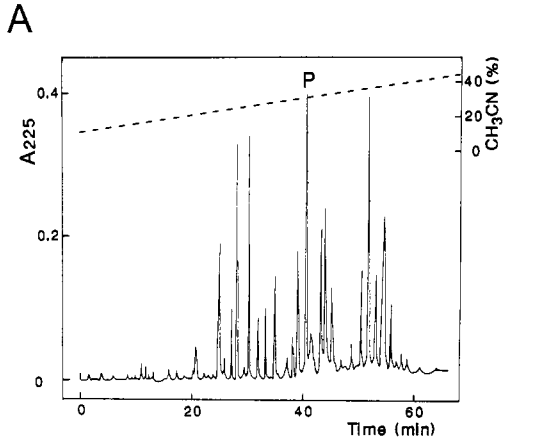

FIGURE 4: Pepsin digestion of Cys-RGD4. (A) Elution pattern of pepsin digests of Cys-RGD4 on reverse-phase HPLC. The pepsin digests of Cys-RGD4 (0.15 mg) were applied to a Shodex ODSpak F-411/S column (0.46 × 10 cm). Elution was performed with a linear gradient of acetonitrile concentration in the presence of 0.1% TFA, at a flow rate of 0.8 mL/min. (B) Identification of fragment P. The fragment P was identified by amino acid analysis and N-terminal sequence analysis. The recovery was estimated to be 95% from the results of the amino acid analysis. The boxed residues indicate the amino acid sequence inserted into human lysozyme. Dots show the positions of Cys residues.

probability = 0.56; (class 2) d = 7.5–8.0 Å; Gly conformation = C* or D*; probability = 0.25; (class 3) d = 5.5–6.0 Å; Gly conformation = C, A*, or B*; probability = 0.06. The letters denoting the conformational regions are indicated in Figure 5D. The classification of the sampled conformations of AVRGDSNA in the same manner showed that classes 1, 2, and 3 in AVCRGDSCNA were sampled 3.7, 1.0, and 0.24 times more frequently than those in AVRGDSNA, respectively. The results suggest that the disulfide bond favors class 1 but suppresses class 3. Typical three-dimensional structures

Table 2: Peptide Mapping Analyses of Fragment P[a]

substrate	protease	product[b]	recovery[c] (%)
fragment P	thermolysin	WĊNDGKTPG	54
		LSĊS (fragment T1)	
		AVĊRGDSĊNAĊH	98
		VAĊ (fragment T2)	
fragment T2	elastase	AVĊRGDSĊNA (fragment E)	75
fragment P	elastase	ĊHLS	78
		VAĊA (fragment E1)	

[a] Protease digestion was carried out under the conditions described in Materials and Methods. Only the fragments containing Cys residues are listed. Dots show the positions of Cys residues. [b] Identified by overall amino acid analysis as well as by the N-terminal amino acid sequence analysis. [c] Estimated from the results of the amino acid analysis.

of these three classes are shown in Figure 5, together with the (ϕ,ψ) angles of Arg, Gly, and Asp. Class 1 has a fully extended Gly structure. Class 2 assumes a type II′ β-turn structure of Gly-Asp with a hydrogen bond between the C=O of Arg and the H–N of Ser. Class 3 is characterized by the proximity of the two side chains of Arg and Asp. Not only the distance d but also the angle between C_α (Arg)–C_β (Arg) and C_α (Asp)–C_β (Asp) is very small; the average angle is 35°. This suggests the presence of a salt bridge between the two side chains of Arg and Asp in class 3.

DISCUSSION

O'Neil et al. (1992) have constructed a phage display library of hexapeptide flanked by two Cys residues, screened the library using the platelet glycoprotein IIb/IIIa (integrin $\alpha_{IIb}\beta_3$), and discovered that CR(or K)GDXXXC- or CXXXR-(or K)GDC-expressing phages can bind tightly to the integrin. More recently, Koivunen et al. (1993) have used a random hexapeptide library expressed on phage, selected various sequences with affinity for fibronectin receptor (integrin $\alpha_5\beta_1$), and found the CRGDCL sequence among them. These results suggest that the introduction of a conformational constraint into the RGD sequence produces a phage coat protein with higher affinity to integrins, although the presence of a disulfide bond between the two Cys residues on both sides of the RGD region was not confirmed in the phage coat protein. In addition, it is known that the cyclic form of an RGD-containing

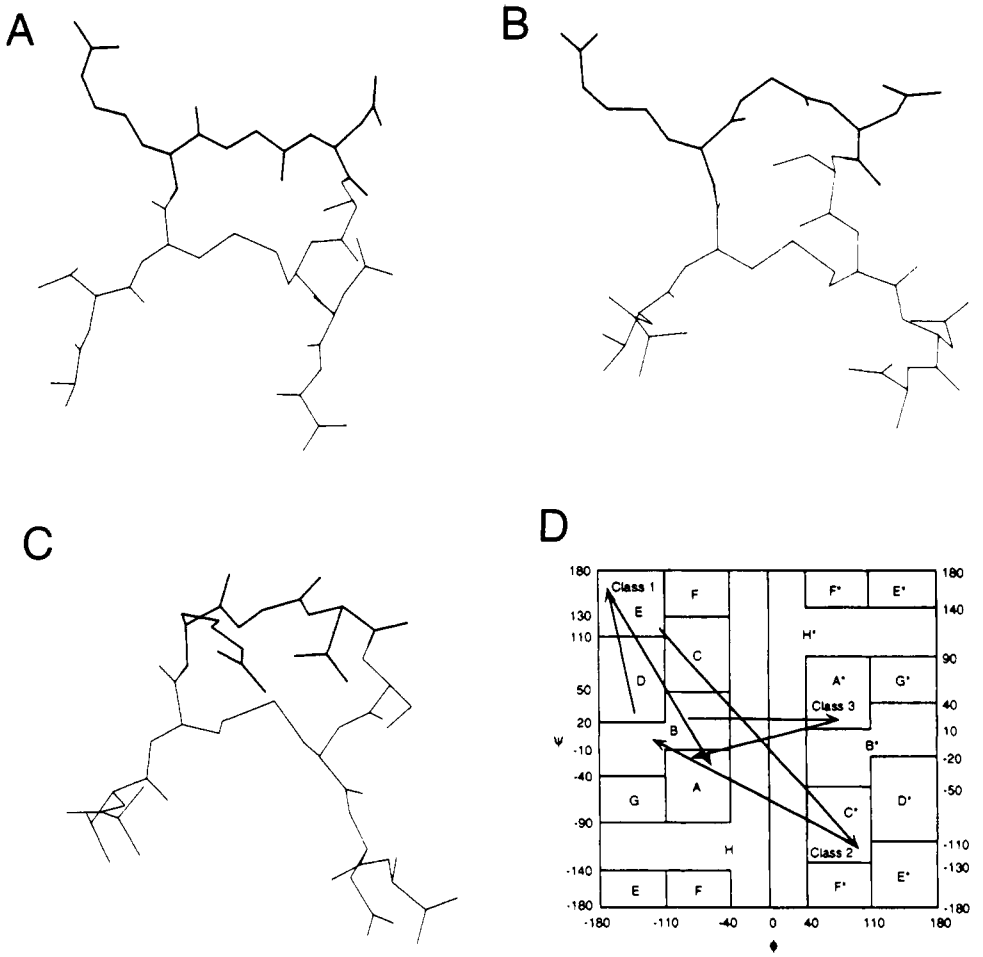

FIGURE 5: Typical three-dimensional structures of AVCRGDSCNA in class 1 (A), class 2 (B), and class 3 (C). All non-hydrogen atoms are shown. The RGD part is indicated by thick lines. (D) (ϕ,ψ) angles of Arg, Gly, and Asp. The (ϕ,ψ) angles of RGD in each class are joined by a line. The structural regions are designated according to the report of Zimmerman et al. (1977).

peptide has much higher affinity to integrins than the linear counterpart (Pierschbacher & Ruoslahti, 1987; Kumagai et al., 1991).

We have constructed three mutant lysozymes, Cys-RGD3, Cys-RGD4, and Cys-RGD5, containing an RGD sequence flanked by two Cys residues, in which CRGDC, CRGDSC, and CGRGDSC, respectively, are inserted between Val74 and Asn75 of human lysozyme. Peptide mapping and mass spectrometric analyses have indicated that these mutant lysozymes possess a new disulfide bond between the two inserted Cys residues, in addition to the four native disulfide bonds of human lysozyme. Human lysozyme consists of two folding domains, the α-helical domain and the β-sheet domain, like hen egg lysozyme (Miranker et al., 1991), and is able to tolerate the packing of mutated polypeptides in the β-sheet domain in *in vivo* folding (Kanaya et al., 1993). Moreover, the long loop from Cys65 to Cys81 in the β-sheet domain, in which the RGD sequence is inserted, is formed during the final step of the folding process of human lysozyme. On the basis of these observations, the correct folding of the present mutants might be reasonable.

Cell adhesion assay using BHK cells has shown that the cell adhesion signals in these mutant lysozymes are transduced to cells through interaction with vitronectin receptor (integrin $\alpha_v\beta_3$) and that these mutants exhibit 2–3-fold higher activity than that of the RGDS-inserted mutant, RGD4. In addition, the inhibitory effects of these mutants on the binding of human fibrinogen to its receptor (integrin $\alpha_{IIb}\beta_3$) have increased in parallel with their adhesion activities to BHK cells. These results demonstrate that the introduction of a conformational constraint into the RGD sequence of the mutant lysozymes significantly increases the affinity for the integrins, as is the case for an RGD-containing peptide. This view would be further supported by the fact that the Cys-RGD5 protein, which is expected to possess an RGD region with a less conformational constraint, exhibits lower cell adhesion activity than those of the Cys-RGD3 and Cys-RGD4 proteins. We previously described that the RGD-containing regions of cell adhesive lysozymes are highly flexible and that such flexibility could allow the conformation of the RGD regions to be induced to fit into the binding pocket of the integrin receptor (Yamada et al., 1993). It is also known that the functional RGD region is conformationally flexible, even in the cases of disintegrins (Adler et al., 1991; Saudek et al., 1991) and the fibronectin type III domain expressed in *Escherichia coli* (Leahy et al., 1992) or in yeasts (Main et al., 1992). Our present results might appear to be inconsistent with these facts. However, it is conceivable that the RGD region, which is highly flexible by nature, assumes a fixed conformation when it binds to integrins to form a ligand–receptor complex. Thus it seems likely that the structures of the RGD regions in the present mutant lysozymes bear a close resemblance to the fixed conformation with biological functions.

The three structural classes of RGD found in the Monte Carlo simulation of AVCRGDSCNA have actually been observed in several experimental studies. The class 1 conformation is found in RGD-containing cyclic disulfides studied by NMR and crystallography (Kopple et al., 1992)

and in the NMR solution structure of flavoridin, one of the disintegrins (Senn & Klaus, 1993). The crystal structure of RGD4 also reveals a class 1 conformation (Yamada et al., 1993). The class 2 conformation is seen in the crystal structure of the fibronectin type III domain (Leahy et al., 1992), which contains the RGD sequence in a type II′ β turn. An NMR study of CRGDC with a disulfide bond (Bogusky et al., 1992) suggests the presence of a salt bridge between Arg and Asp, the typical feature of class 3. In principle, none of these conformations can be ruled out from the model structure of AVCRGDSCNA. However, two lines of evidence, the large probability of occurrence in the simulation and the crystal structure of RGD4, suggest that the most probable conformation of AVCRGDSCNA belongs to class 1 with an extended Gly residue.

ACKNOWLEDGMENT

We thank Drs. M. Ikehara and K. Sekiguchi for their interest and encouragement throughout this work. We also wish to thank Drs. T. Takao and Y. Shimonishi for mass spectrometric analyses.

REFERENCES

Adler, M., Lazarus, R. A., Dennis, M. S., & Wagner, G. (1991) *Science 253*, 445–448.

Bogusky, M. J., Naylor, A. M., Pitzenberger, S. M., Nutt, R. F., Brady, S. F., Colton, C. D., Sisko, J. T., Anderson, P. S., & Verber, D. F. (1992) *Int. J. Pept. Protein Res. 39*, 63–76.

Charo, I. F., Nannizzi, L., Phillips, D. R., Hsu, M. A., & Scarborough, R. M. (1991) *J. Biol. Chem. 266*, 1415–1421.

Ellman, G. L. (1959) *Arch. Biochem. Biophys. 82*, 70–77.

Fitzgerald, L. A., Leung, B., & Phillips, D. R. (1985) *Anal. Biochem. 151*, 169–177.

Hemler, M. E. (1991) in *Receptors for Extracellular Matrix* (McDonald, J. A., & Mecham, R. P., Eds.) pp 255–300, Academic Press, San Diego, CA.

Hynes, R. O. (1987) *Cell 48*, 549–554.

Inaka, K., Taniyama, Y., Kikuchi, M., Morikawa, K., & Matsushima, M. (1991) *J. Biol. Chem. 266*, 12599–12603.

Kanaya, E., & Kikuchi, M. (1992) *J. Biol. Chem. 267*, 15111–15115.

Kanaya, E., Ishihara, K., Tsunasawa, S., Nokihara, K., & Kikuchi, M. (1993) *Biochem. J. 292*, 469–476.

Kieffer, N., Fitzgerald, L. A., Wolf, D., Cheresh, D. A., & Phillips, D. R. (1991) *J. Cell Biol. 113*, 451–461.

Kikuchi, M., Taniyama, Y., Kanaya, S., Takao, T., & Shimonishi, Y. (1990) *Eur. J. Biochem. 187*, 315–320.

Koivunen, E., Gay, D. A., & Ruoslahti, E. (1993) *J. Biol. Chem. 268*, 20205–20210.

Kopple, K. D., Baures, P. W., Bean, J. W., D'Ambrosio, C. A., Hughes, J. L., Peishoff, C. E., & Eggleston, D. S. (1992) *J. Am. Chem. Soc. 114*, 9615–9623.

Kumagai, H., Tajima, M., Ueno, Y., Giga-Hama, Y., & Ohba, M. (1991) *Biochem. Biophys. Res. Commun. 177*, 74–82.

Leahy, D. J., Hendrickson, W. A., Aukhil, I., & Erickson, H. P. (1992) *Science 258*, 987–991.

Maeda, T., Oyama, R., Ichihara-Tanaka, K., Kimizuka, F., Kato, I., Titani, K., & Sekiguchi, K. (1989) *J. Biol. Chem. 264*, 15165–15168.

Main, A. L., Harvey, T. S., Baron, M., Boyd, J., & Campbell, I. D. (1992) *Cell 71*, 671–678.

Miranker, A., Radford, S. E., Karplus, M., & Dobson, C. M. (1991) *Nature 349*, 633–636.

Noguti, T., & Gō, N. (1985) *Biopolymers 24*, 527–546.

O'Neil, K. T., Hoess, R. H., Jackson, S. A., Ramachandran, N. S., Mousa, S. A., & DeGrado, W. F. (1992) *Proteins: Struct., Funct., Genet. 14*, 509–515.

Pierschbacher, M. D., & Ruoslahti, E. (1984) *Nature 309*, 30–33.

Pierschbacher, M. D., & Ruoslahti, E. (1987) *J. Biol. Chem. 262*, 17294–17298.

Ruoslahti, E., & Pierschbacher, M. D. (1987) *Science 238*, 491–497.

Saudek, V., Atkinson, R. A., & Pelton, J. T. (1991) *Biochemistry 30*, 7369–7372.

Senn, H., & Klaus, W. (1993) *J. Mol. Biol. 232*, 907–925.

Sippl, M. J., Némethy, G., & Scheraga, H. A. (1984) *J. Phys. Chem. 88*, 6231–6233.

Suzuki, S., Oldberg, A., Hayman, E. G., Pierschbacher, M. D., & Ruoslahti, E. (1985) *EMBO J. 4*, 2519–2524.

Taniyama, Y., Yamamoto, Y., Nakao, M., Kikuchi, M., & Ikehara, M. (1988) *Biochem. Biophys. Res. Commun. 152*, 962–967.

Taniyama, Y., Yamamoto, Y., Kuroki, R., & Kikuchi, M. (1990) *J. Biol. Chem. 265*, 7570–7575.

Wako, H., & Gō, N. (1987) *J. Comput. Chem. 8*, 625–635.

Watt, K. W. K., Cottrall, B. A., Strong, D. D., & Doolittle, R. F. (1979) *Biochemistry 18*, 5410–5416.

Yamada, T., Matsushima, M., Inaka, K., Ohkubo, T., Uyeda, A., Maeda, T., Titani, K., Sekiguchi, K., & Kikuchi, M. (1993) *J. Biol. Chem. 268*, 10588–10592.

Yamada, T., Uyeda, A., Otsu, M., Matsushima, M., Sekiguchi, K., & Kikuchi, M. (1994) *Biochemistry 33*, 3885–3889.

Yoshimura, K., Toibana, A., Kikuchi, K., Kobayashi, M., Hayakawa, T., Nakahama, K., Kikuchi, M., & Ikehara, M. (1987) *Biochem. Biophys. Res. Commun. 145*, 712–718.

Zimmerman, S. S., Pottle, M., Némethy, G., & Scheraga, H. A. (1977) *Macromolecules 10*, 1–9.